Energy dissipation regarding transient response of concrete structures

Constitutive equations coupling damage and friction

Frédéric Ragueneau* — Jacky Mazars* — Christian La Borderie**

**Laboratoire de Mécanique et technologie, ENS de Cachan - CNRS UMR 8535/Université Pierre et Marie Curie*
61, avenue du président Wilson, F-94235 Cachan cedex
ragueneau@lmt.ens-cachan.fr

*** LaSAGeC, ISA du BTP, Université de Pau et des Pays de l'Adour*
1, allée Cantau, F-64600 Anglet

ABSTRACT. *This paper deals with the 3D expression of a constitutive relation for brittle materials such as concrete accounting for cracking with friction. Based on damage mechanics, a macroscopic description of the material behaviour introducing this new dissipative phenomenon allows one to take into account, during cyclic loading, the hysteresis loops at a fixed level of damage. This model has been implemented within a multilayered finite element code dedicated to the analysis of structures subjected to seismic loading. First computations enlighten the role of an accurate description of the material physical dissipation towards the global damping at the structural level.*

RÉSUMÉ. *Le présent article a pour objet de présenter un modèle de comportement tridimensionnel pour matériaux fragiles tels que le béton prenant en compte le mécanisme de fissuration avec frottement. Fondée sur la mécanique de l'endommagement, une description macroscopique du comportement introduisant un nouveau phénomène dissipatif (résultant de la rugosité des fissures) permet de décrire la présence de boucles d'hystérésis à un niveau fixe d'endommagement lors de chargements cycliques. Ce modèle a été implanté dans un code de calculs aux éléments finis multicouches permettant de traiter des problèmes de structures soumis au risque sismique. Des analyses comparant les différentes énergies mises en jeu permettent de mettre en évidence l'importance d'une description physique des diverses sources de dissipation locale dans la représentation de l'amortissement global à l'échelle de la structure.*

KEY WORDS: *concrete, damage, sliding with friction, damping, seismic.*

MOTS-CLÉS : *béton, endommagement, glissement avec frottement, amortissement, sismique.*

1. Introduction

Transient non-linear computations of structures need the use of energy dissipation tools for both physical and numerical reasons. One of the major drawbacks in such analysis lies in the expression of the damping matrix. Several kinds of methods can be used to achieve that purpose, such as viscous or hysteretic [BAT 82]. A more realistic approach consists in a better modelling of the internal dissipation. Recent experiments on reinforced concrete mock-up subjected to seismic loading permitted to appreciate the strong interaction between state of failure and resulting global damping [QUE 98]. Most of the constitutive models are able to reproduce realistically the behaviour of concrete in the non-linear range, based on damage mechanics, on plasticity theory or using the microplane concept [JU 89] [KRA 81]. They often ensure predictive computations in the static case but do not easily take into account a main cyclic characteristic: the influence of heterogeneities and roughness of the crack surfaces. At a fixed level of damage, concrete still exhibits dissipation due to the frictional sliding between crack surfaces. This property can be experimentally observed for a specimen during cyclic solicitations through the hysteresis loops.

A new constitutive relation for concrete material including residual hysteretic loops at a fixed level of damage is proposed. Derived from the thermodynamics framework, it allows to couple the state of cracking with the hysteretic dissipation induced by the crack surfaces sliding. Based on damage mechanics, a particular Helmholtz free energy allows to introduce a coupling of the level of damage in one direction to a frictional stress. The main assumption postulated to describe the hystereretic behaviour is that cracks surfaces created after fracture will not open anymore following a perfect surface but will slide considering their roughness. This phenomenon induces the occurrence of a sliding stress which prevents the crack from going on opening easily. In other sense, the consumed energy during cracking is not entirely dissipated but part of it is stored in a the sliding potential. This frictional stress ($\boldsymbol{\sigma}_s$) is assumed to have a plasticity-like behaviour associated with a non-linear kinematic hardening. A particular dissipative potential allows the description of dilatancy, fundamental feature of geo-materials like concrete, sand or rocks.

This model has been implemented in the finite element code EFICOS based on a multilayered beam kinematics approach. Concerning the constitutive equations, we choosed the implicit return mapping algorithm. This approach of structural computation allows to take into account at the local level refined material models, avoiding at the same time heavy analysis. In order to validate our approach of structural dissipation, comparisons between computations and experiments are shown. This communication focuses on the 3D expression of the local model and on numerical comparisons of energy dissipation at the structural level pointing out the influence of frictional sliding regarding global damping.

2. Crack growth and damage

2.1. *State potential*

Initially introduced by Kachanov [KAC 58] for creep failure problems, the damage mechanics formulation requires the addition of a new internal variable in order to represent the macroscopic loss of stiffness [LEM 90]. This can be achieved in many ways. The classical one is to relate the damaged material's and the intact material's elastic properties. Defining a damage variable requires reducing the rank of damage operator while maintaining as well as can be the experimental properties of the material. In order to reach this objective, the effective stress concept is introduced. It induces a relation between the stress tensor and the effective stress tensor through a strain equivalence (the effective stress which, when applied to the undamaged material, produces the same strain).

Therefore, in the basic form, a scalar variable can be used for the sake of simplicity. Numerous authors have proposed several expressions of different ranks for the damage variable. The fourth-order tensor was suggested by Chaboche. Second-order tensors are more frequently introduced [DRA 94]. In this case, a problem exists in that the symmetry of the elasticity operator is no longer insured, as it depends on the way one defines the previous relation [MUR 78]. Cordebois [COR 79] postulated a state potential which depends only on the effective stress. Therefore, the symmetry of the elasticity operator is obtained through this energy equivalence.

The pursuit of a physical and realistic description of the oriented crack growth in concrete without neglecting the simplicity requirement led to a second-order damage tensor formulation. In order to make the subsequent numerical implementation of the model in a finite element code easier, Helmholtz's strain-based free energy has been chosen. Considering a particular definition for the damage variable $\boldsymbol{d}$, an effective strain tensor is defined on the principal axis of the damage tensor as follows,

$$\tilde{\varepsilon} = (1-d)^{1/4} . \varepsilon . (1-d)^{1/4} \qquad [1]$$

Where $\tilde{\varepsilon}$ is the effective strain tensor, ε the second order strain tensor (symmetric part of the displacement gradient field) and $\boldsymbol{d}$ the symmetric second order tensor related to damage phenomena. Because of symmetry conditions on the resulting stress tensor, the expression in the previous relation denotes a symmetrization. This effective strain, introduced directly into the state potential, allows for the description of an elasto-damage material exhibiting orthotropic cracks:

$$\rho\psi_d = \frac{1}{2}\left\{2\mu\tilde{\varepsilon} : \tilde{\varepsilon} + \lambda Tr^2\left[\tilde{\varepsilon}\right]\right\} \qquad [2]$$

with μ and λ, the Lamé coefficients defined for the undamaged material. ρ is the material density and ψ_d is the Helmoltz's free energy.

2.2. *Damage criteria and evolution laws*

Based on experimental investigations, damage for brittle materials such as concrete is governed principally by their tensile behavior. To take into account this asymmetry, two damage tensors must be introduced. The splitting between the tensile and the compressive damage tensors is achieved through the sign of the sliding strains (defined in the next section) expressed in their respective principal directions:

$$\boldsymbol{d} = \boldsymbol{d}^{+}\boldsymbol{H}^{+}(\boldsymbol{\varepsilon}_s) + \boldsymbol{d}^{-}\boldsymbol{H}^{-}(\boldsymbol{\varepsilon}_s) \qquad [3]$$

With $\boldsymbol{H}^{+}(\boldsymbol{\varepsilon}_s) = \boldsymbol{P}^{-1}\boldsymbol{H}(\boldsymbol{\lambda})\boldsymbol{P}$ and $\boldsymbol{H}^{-}(\boldsymbol{\varepsilon}_s) = \boldsymbol{P}^{-1}\boldsymbol{H}(\boldsymbol{1}-\boldsymbol{\lambda})\boldsymbol{P} = \boldsymbol{1} - \boldsymbol{H}^{+}(\boldsymbol{\varepsilon}_s)$ (tensorial functions), $\boldsymbol{\lambda}$ is the tensor of strain eigenvalues and $\boldsymbol{P}$ the transformation matrix. $\boldsymbol{H}$ is the Heaviside function.

The level of damage is governed by the value of positive strains. The evolution equation assumed to be expressed in its incremental form as follows, is written in the principal axes of the incremental strains:

$$\dot{d}_i^{+} = \left[\frac{\varepsilon_{d0}}{\varepsilon_i^{+2}} \left(1 + \varepsilon_i^{+} Bt\right) \exp\left(Bt\left(\varepsilon_{d0} - \varepsilon_i\right)\right) \right] \dot{\varepsilon}_i^{+} \qquad [4]$$

Bt is a material parameter driving the slope of the softening branch. The associated damage criterion is also expressed in the principal axis of the strain tensor:

$$f_i = \varepsilon_i - \varepsilon_{d0} - \kappa(\varepsilon_i) \qquad [5]$$

ε_{d0} is the initial tensile yield strain, usually equal to 1.10^{-04}. $\kappa(\varepsilon_i)$ is the hardening variable. Such a criterion is similar to the so-called St-Venant's criterion in the principal stress space.

The use of a damage evolution law based on the state of total strain is coherent with the meaning of the damage variable expressed in the elasticity law.

Compressive damage in a particular direction is considered only as a consequence of the tensile behavior of the material and, therefore, is taken equal to a function of the state of tensile cracking along the orthogonal directions.

$$d_i^- = \left(\frac{d_j^+ + d_k^+}{2} \right)^{\beta} \qquad [6]$$

β is a material parameter connecting the damaged Young's moduli for two orthogonal directions. The comparison of apparent Young's moduli in the longitudinal and radial directions allows the measurement of β.

3. Inelasticity and friction coupled to damage

3.1. *State potential*

The main assumption used to describe the hysteretic behavior is that crack lips arising from fracture do not open further along a perfect surface but slide depending on their rugosity. This phenomenon induces a sliding stress which prevents the crack from continuing to open easily. In other terms, the energy consumed during cracking is not entirely dissipated but part of it is stored in the sliding potential. Thus, this is through the damage variable that this energy shift can be obtained. Each dissipative nonlinear phenomena needing its own internal variable, a measure of the sliding with friction will be defined thanks to a particular second order new variable: the sliding strain ε_s. Following the same methodology as in section 2, sliding is integrated into the behavior through an equivalent strain which couples damage and elasticity of the sliding surface.

$$\hat{\varepsilon} = \boldsymbol{d}^{1/4}.(\varepsilon - \varepsilon_s)\boldsymbol{d}^{1/4} \qquad [7]$$

In that way, the total state potential is written as follows,

$$\rho\psi = \rho\psi_d(\tilde{\varepsilon}) + \rho\psi_s(\hat{\varepsilon}), \text{ with } \rho\psi_s = \frac{1}{2}\left\{2\mu\hat{\varepsilon} : \hat{\varepsilon} + \lambda Tr^2[\hat{\varepsilon}]\right\} + \frac{1}{2}b\alpha : \alpha \qquad [8]$$

α is the internal variable associated with the kinematic hardening phenomenon and b is a material parameter.

One can easily recognize a classical elasto-damage coupling and a new term allowing the energy to shift from the elasto-damageable part to the frictional sliding part. The coupling between sliding and cracking is made possible thanks to the presence of the damage variable as a multiplier in the second element of the right-hand side of [8].

3.2. *State laws*

In order to define the state laws, the model has to be thermodynamically admissible: it must comply with the positiveness of the dissipated energy. Starting from the Clausius-Duhem inequality, and assuming that the state potential is linearized around the current value of every state variable, the state laws are expressed as follows:

The stress tensors can be derived as,

$$\sigma = \rho \frac{\partial \psi}{\partial \varepsilon} = 2\mu(1-d)^{1/2}.\varepsilon.(1-d)^{1/2} + \lambda(1-d)^{1/2} Tr\left[\varepsilon.(1-d)^{1/2}\right] + 2\mu d^{1/2}.(\varepsilon - \varepsilon_s).d^{1/2} + \lambda d^{1/2} Tr\left[(\varepsilon - \varepsilon_s).d^{1/2}\right] \quad [9]$$

And the sliding stress tensor, associated to the sliding strain:

$$\sigma_s = -\rho \frac{\partial \psi}{\partial \varepsilon_s} = 2\mu d^{1/2}.(\varepsilon - \varepsilon_s).d^{1/2} + \lambda d^{1/2} Tr\left[(\varepsilon - \varepsilon_s).d^{1/2}\right] \quad [10]$$

The back stress is defined as:

$$X = \rho \frac{\partial \psi_s}{\partial \alpha} = b\alpha \quad [11]$$

We can observe that the total stress is divided into two parts: a classical elasto-damage component and a sliding component. Damage is classically controlled by the elasto-damage stress and the sliding strain is linked only to the sliding part of the stress. This kind of partitioning, in conjunction with the two failure surfaces, allows the description of a hysteretic behavior at a fixed level of damage. Details on the complementary and evolution laws will be developed in the next section. At this description level, such an approach could be compared to multi-surface modeling [MRO 67], except for the fact that the surfaces are not expressed in the same space (strain space for damage and stress space for sliding). The sliding and plastic strains being different, the thermodynamic forces associated with the total strain and the sliding strain are different. Such a formulation differs greatly from the classical plasticity-damage coupling. This choice of introducing damage into the sliding stress is guided by the idea that all inelastic phenomena in concrete result from the cracks' growth. The thermal aspects are presently ignored.

3.3. *Sliding criteria and plastic potential*

The sliding part of the constitutive relation is assumed to represent a plasticity-like behavior. In order to reproduce the hysteresis loops, nonlinear kinematic hardening is considered. Initially introduced by Armstrong & Frederick [ARM 66] and recently developed further [CHA 93], it allows the formulation to overcome the major drawback of Prager's kinematic hardening law, *i.e.* the linearity of the state law defining the forces associated with kinematic hardening. The nonlinear terms are added in the dissipative potential. The sliding criterion takes the classical form:

$$f = J_2(\sigma_s - X) - \sigma_y \leq 0 \qquad [12]$$

$J_2(\sigma_s - X)$ *i.e.* Von Mises' equivalent stress was chosen to a first approximation in order to keep simplicity and adequacy to classical numerical algorithm for constitutive laws implementation. The specific aspects of geo-materials non-linear behaviour have been introduced in the plastic potentials

Classical plasticity, in order to govern the evolution of the internal variables, requires the definition of a dissipative potential. The expectation of nonlinear kinematic hardening imposes the use of a non-associated flow rule:

$$\phi = J_2(\sigma_s - X) + \frac{3}{4} aX : X + cI_I - \sigma_y \qquad [13]$$

With $I_1 = \frac{1}{3} Tr[\sigma_s]$, the first invariant of the sliding stress tensor. It enables one to take into account the dilatancy phenomenon observed experimentally on geomaterials such as concrete or rocks. a and c are material parameters. As a result of the normality rules, the evolution laws of the internal variables are expressed as follows, thus insuring that the dissipation is positive:

$$\dot{\varepsilon}_s = \dot{\lambda} \frac{\partial \phi}{\partial \sigma_s} \text{ and } \dot{\alpha}_s = -\dot{\lambda} \frac{\partial \phi}{\partial X} \qquad [14]\,[15]$$

$\dot{\lambda}$ is the plastic multiplier, determined by the consistency condition.

3.4. *Unilateral effects*

In the case of cyclic loading, a model has to take into account the crack closure phenomenon which generates the concurrent stiffness recovery. Some damage models have been extended to take into account the crack closure conditions by inducing different behaviors in tension and in compression. A general and rigorous framework concerning the unilateral condition, based on a particular decomposition of the elastic energy introducing a deviatoric behavior and a spherical one, is given by Ladevèze [LAD 83]. Other kinds of anisotropic damage models based on a mesocrack description can also deal with the crack closure condition [HAL 96].

In our case, the need to couple damage with sliding of the crack surfaces led us to the introduction of a second-order damage tensor. This was achieved through a particular effective strain [1] [7] introduced into the elastic free energy for the damage part as well as for the sliding part. This enables a physical description of the material behavior (oriented cracking, inelasticity, nonlinear unloading) but is not in good agreement with the unilateral condition. This is due to the presence of tensorial damage in the volumetric part of the stress [9]. Concerning the radial loading cases in our analysis, a simplification of the previous model has to be achieved. The same formulation is retained, but an isotropic evolution of the damage tensors is now assumed. For the damage part, the simplified model boils down to two scalar damage variables allowing to account for stiffness restoring after tensile degradation keeping in the same time the continuity of the stress-strain law. The figure 1 shows the response of the model subject to crack closure following a tensile loading path:

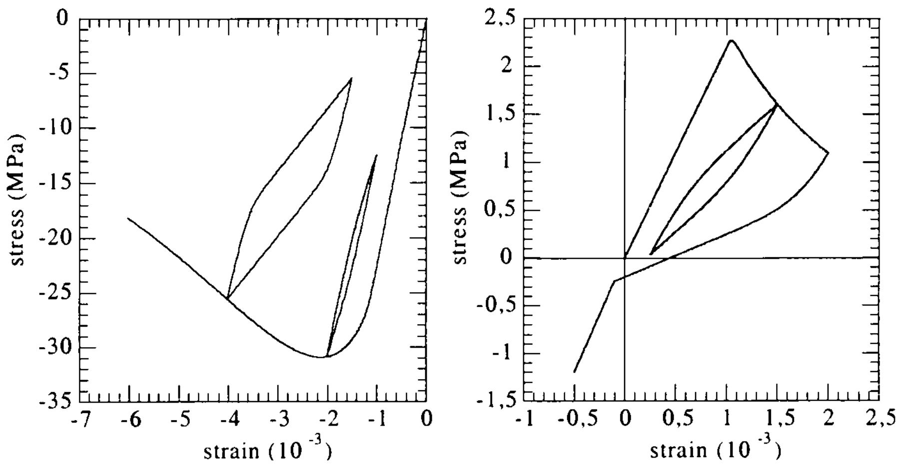

Figure 1. *Compression/Tension response. Unilateral effect and stiffness recovery. The thickness of the hysteresis loops is proportional to the state of cracking*

4. Numerical implementation

4.1. *Finite element code: EFiCoS*

The choice of using a multilayered f.e. configuration combines the advantage of using beam type finite elements with the simplicity of uniaxial behavior. Each finite element is a beam which is discretized into several layers. The basic assumption is that plane sections remain plane (Bernoulli's kinematic) allowing to consider a uniaxial behavior of each layer. The local constitutive equations are integrated for each layer of a cross section. Concerning reinforced concrete structures, reinforcement steel bars are introduced with special layers, the behavior of which is a combination of those of concrete and steel. A mixing homogenized law is considered.

For each element a secant matrix $\boldsymbol{K}$ is assembled from the relation between $\boldsymbol{\sigma}$ and $\boldsymbol{\varepsilon}$. The non-linear behaviors appear in the second member of the equilibrium equation and are subtracted from the vector of generalized forces:

$$KU = F_{ext} - F_{in} \qquad [16]$$

In which U is the vector of nodal displacements, F_{ext} is the vector of external forces and F_{in} is the vector of inelastic forces. Such a formulation, based on the initial secant stiffness matrix algorithm is well suited to our modeling. After reaching the peak-load, it prevents the iteration matrix from becoming singular. Concerning dynamic analysis, the same framework is used. The seismic loading is applied by the mean of an accelerogram at the basis of the structure. A double integration of this signal allows to determine the ground displacement. In such way, the equations of motions are solved in the global coordinates and allow to deal with computations needing different accelerograms exciting different parts of a same structure at the same time. For stability and precision reasons, a classical Newmark algorithm has been implemented to solve the equation of motion [NEW 59]. The expression of the discretized displacements and celerities are derived as:

$$\dot{U}_{t+\Delta t} = \dot{U}_t + \left[(1-\gamma)\ddot{U}_t + \gamma\ddot{U}_{t+\Delta}\right]\Delta t \qquad [17]$$

$$U_{t+\Delta t} = U_t + \Delta t\dot{U}_t + \left[\left(\frac{1}{2} - \beta\right)\ddot{U}_t + \beta\ddot{U}_{t+\Delta}\right]\Delta t^2 \qquad [18]$$

Choosing $\gamma = 1/2$ and $\beta = 1/4$ prevent us from any numerical dissipation and ensures an unconditional scheme stability. This expressions are introduced in the equations of motions at step $t + \Delta t$ imposing an implicit integration scheme.

4.2. *Constitutive law implementation*

By defining two different surfaces, one can integrate the damage tensor under traction explicitly. For uniaxial compression, the algorithm becomes implicit due to the dependence of the compressive damage on the radial extension, in which case a kind of plane stress procedure has to be introduced. Concerning the sliding stress, a classical implicit analysis has to be carried out. Among the different methods available for this purpose (Euler's backward or mid-point rules algorithm solved by an iterative Newton method), we chose the classical form of the so-called "return mapping" algorithm [ORT 86]. Indeed, it ensures convergence in the most efficient way. More details concerning the numerical implementation can be found in [RAG 00].

5. Applications

5.1. *Response to uniaxial stress loading*

The analysis is performed at the material level. Figure 3 represents the simulation of the uniaxial compression test. One can observe that the model is able to describe the volumetric response of the material satisfactorily. The material parameters used for the analysis are: E = 36 000 MPa, $\nu = 0.24$, $\varepsilon_{d0} = 1.10^{-04}$, $Bt_{direct} = 9\ 000$, $Bt_{induced} = 300$, $\beta = 12$, $a_{direct} = 5.0\ 10^{-06}\ MPa^{-1}$, $b_{direct} = 1.0\ 10^{+10}$ MPa, $a_{induced} = 2.0\ 10^{-08}\ MPa^{-1}$, $b_{induced} = 1.0\ 10^{+10}$ MPa, c = 0.18. The direct and induced qualification are related to the cracking mode: direct means that frictional stress and damage are aligned with the direction of loading.

The two curves in Figure 1 show the ability of the model to describe the hysteresis loops under traction and compression loading paths. The hysteretic dissipation capability of the model can be illustrated by plotting the absorbed energy of an unloading tensile loop against the value of tensile damage in Figure 3. One can easily appreciate the effect of the coupling between the state of damage and the sliding stress. Despite the lack of physical shape of the yield surface for the 2D compression state due to the use of a St Venant's-type criterion, the use of an induced and direct damage evolution law allows a good modeling of a 3D state of confinement. Figure 3 shows such an effect induced by a lateral pressure applied proportionally to the longitudinal one (radial path).

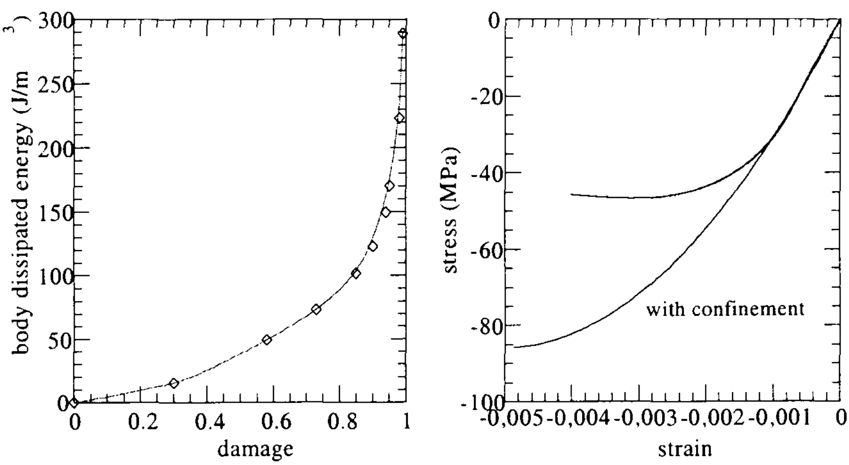

Figure 2. *Dissipated energy versus Damage-Radial confinement effect*

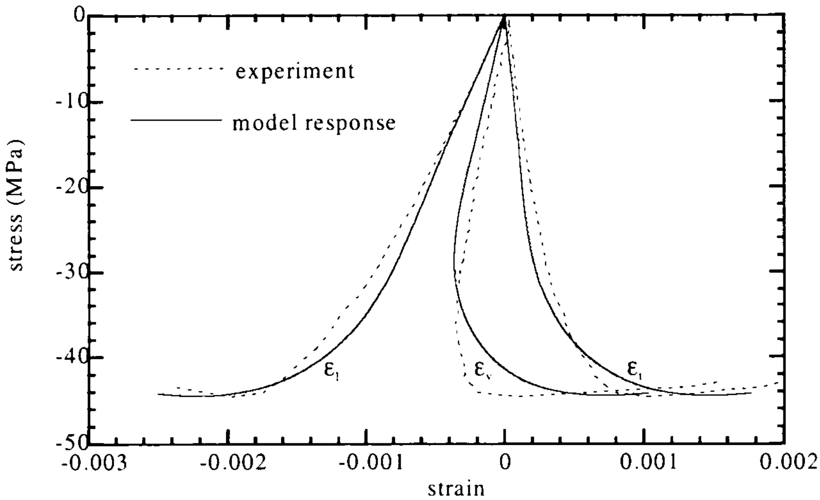

Figure 3. *Compression test simulation, longitudinal, orthogonal and volumetric strain*

5.2. *Structural applications: seismic case study*

This section is dedicated to the contribution of this local material model to the global dissipation at the structural level. A dynamic example of a reinforced concrete mock-up subjected to an earthquake loading confirms the relevance of our local approach in modeling damping in the nonlinear range. The main purpose of the CAMUS experimental program [QUE 98] is to demonstrate the ability of reinforced concrete bearing walls to sustain seismic loading. To reach this goal, a one-third scale model was tested on the shaking table of CEA. This mock-up was composed of two parallel walls connected by 6 square slabs. A heavily reinforced footing allowed the mock-up to be anchored to the shaking table. The mock-up plans are shown below:

The mock-up is loaded through horizontal accelerations parallel to the walls. The presence of steel bracing systems at each level disposed perpendicularly to the loading direction prevents any torsion modes occurrence. The accelerograms are modified in time with a ratio of $1/\sqrt{3}$ to take into account the similarity rules. Two types of accelerogram are imposed: Nice S1 for the far field type earthquake and San-Francisco (earthquake happened in 1957) for the near field one. The response spectra may show the difference of these two kinds of earthquakes: on one hand Nice is very rich in terms of frequencies and on the other hand, San Francisco has a thicker effective band width of high accelerations. The complete experimental sequence, as shown in figure 5, is: Nice 0.25 g, San Francisco 1.13 g, Nice 0.4 g and Nice 0.71 g.

A simple modeling of the boundary conditions at the base was obtained using a horizontal bending beam instead of assuming a perfect anchorage introducing the anchorage and contacts defects. The knowledge of the stiffness measured from the shaking table helped us adjust the vertical stiffness as well as the rotational stiffness of the elements along the boundary. This kind of modeling allowed us to take into account 2 eigenmodes, which is the minimum for a structure such as CAMUS where the second vertical mode plays a major role.

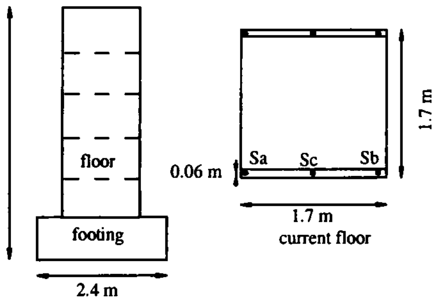

	Sa, Sb	Sc
Level 5	15.9	78.4
Level 4	28.3	78.4
Level 3	94.4	110.2
Level 2	188.9	138
Level 1	289.4	138

Steel reinforcement ratio for each wall (mm2)

Figure 4. *CAMUS Mock-up*

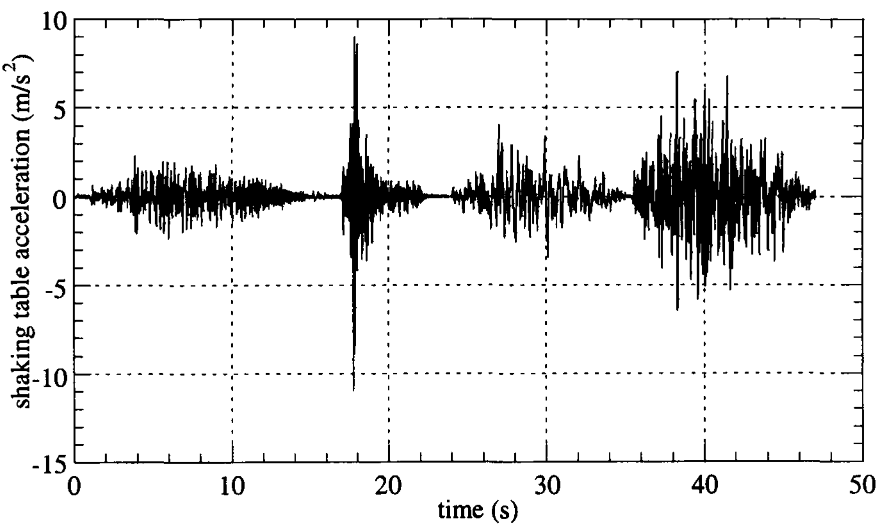

Figure 5. *Accelerograms: experimental complete sequence*

No structural Rayleigh damping was introduced into the analysis. The global behavior of the mock-up was well-reproduced. The benefit of such a material modeling is made more obvious by focusing our comparisons on energy balance.

Figure 6 and 7 shows comparisons between the new model with no viscous damping and a classical damage model [LAB 91] with Rayleigh damping in terms of energy equilibrium.

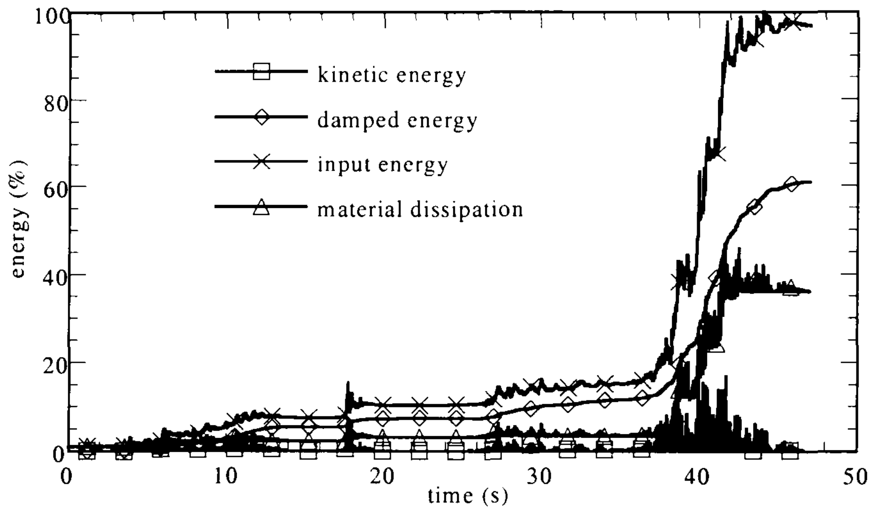

Figure 6. *Computations with a classical damage model: Dissipation through a global viscous matrix*

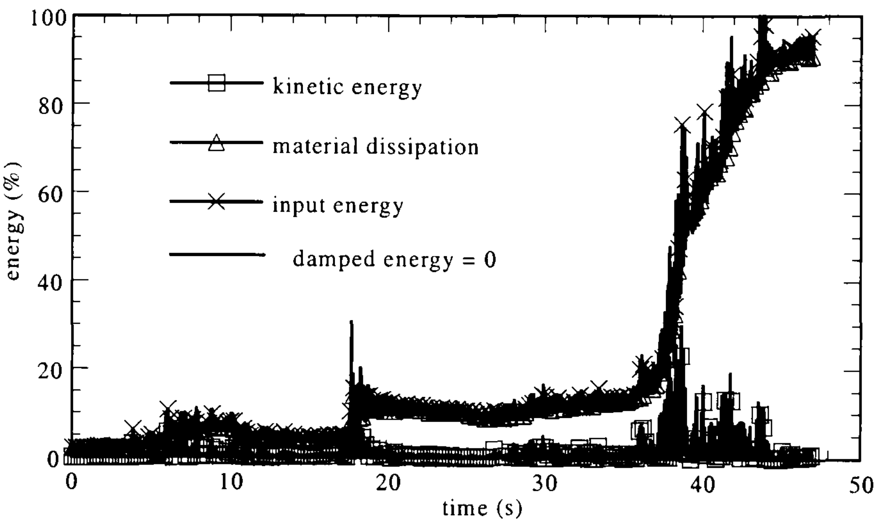

Figure 7. *Hysteretical energy dissipation: Computations without any viscous Rayleigh damping*

We can notice that for a "traditional" model of damage, the external Rayleigh's damping takes part in height of 60 % to the total dissipation of energy. In the case of the second model, all energy is dissipated within material. From a quantitative point of view, no adjustment is necessary at the level of the structural analysis and from a qualitative point of view, dissipation is relocated in the zones of strong degradations (in the three lowest level) and no more distributed on the whole of the structure.

6. Conclusions

Analyzing a specific case study (the response of a reinforced concrete model subjected to seismic loading) allowed us to point out the major features of local non-linear mechanisms which should be integrated in the analysis. Local constitutive equations based on damage mechanics for concrete have been developed and implemented in a finite element code dedicated to civil engineering large scale computations. The use of simplified finite element method, allowing parametrical studies, helped us to understand and analyse the experimental responses by pointing out the influences of physical material features such as frictional sliding between crack faces This approach of damage mechanics coupling cracking and frictional sliding emphasizes the importance of a refine material modeling with regards to the accuracy and the predictive ability of structural computation tools. The effect of modelling the hysteresis loops was analyzed through its contribution to overall damping. The use of this kind of local model for dynamic and, in particular, seismic loading may, in the non-linear range, make the explicit expression of an often arbitrarily-defined damping matrix unnecessary. The role played by this global viscous damping matrix in the analysis is considerably lessened. More investigations in the identification of material parameters at the specimen scale subjected to complex loading paths would allow to treat the cases of 3D structures bearing complex solicitations combining shear and torsion effects.

7. References

[ARM 66] ARMSTRONG P.J. and FREDERICK C.O., A Mathematical Representation of the Multiaxial Bauschinger Effect, G.E.G.B., Report RD/B/N, 731, 1966.

[BAT 82] BATHE K.J., *Finite element procedures in engineering analysis,* Prentice Hall (eds), Inc. Englewood Cl.iffs, New Jersey, 1982.

[CHA 93] CHABOCHE J.L., "Cyclic Viscoplastic Constitutive Equations, Part I: A Thermodynamically Consistent formulation", *J. Appl. Mech.*, Vol 60, p. 813-821, Dec. 1993.

[COR 79] CORDEBOIS J.P. and SIDOROFF F., "Damage Induced Elastic Anisotropy", *Colloque Euromech*, 115, Villars de Lans, p. 761-774, 1979.

[DRA 94] DRAGON A., CORMERY T., DESOYER T. and HALM D., "Localised Failure Analysis Using Damage Models", In Chambon R. *et al.* (eds), *Localisation and Bifurcation Theory for Soils and Rocks*, p. 127-140. Rotterdam:Balkema, 1994.

[HALM 96] HALM D. and DRAGON A., "A model of anisotropic damage by mesocrack growth; unilateral effect", *In. J. Damage Mechs.*, Vol. 5, Oct. 1996, p. 384-402, 1996.

[JU 89] JU J.W., "On energy-based coupled elastoplastic damage theories: constitutive modelling and computational aspects", *Int. J. Solids and Structures*, 25(7), p. 803-833, 1989.

[KAC 58] KACHANOV L.M., "Time of the rupture process under creep conditions", *Izv. Akad. Nauk. S.S.R.*, Otd. Tekh. Nauk., n° 8, p. 26-31, 1958.

[KRA 81] KRACJINOVIC D. et FONSEKA G.U., "The continuous damage theories of brittle materials, Part I and II", *J. of Appl. Mech.*, ASME, Vol. 48, p. 809-824, 1981.

[LAB 91] LA BORDERIE CH., Phénomènes unilatéraux dans un matériau endommageable: modélisation et application à l'analyse de structures en béton, Ph. D. thesis, Univ. Paris VI, 1991.

[LAD 83] LADEVÈZE P., "On an anisotropic damage theory", *Proc. CNRS Int. Coll.* 351, Villars-de-Lans, Ed. by J.P. Boehler, p. 355-363, 1983.

[LEM 90] LEMAITRE J. and CHABOCHE J.L., *Mechanics of solids material*, Cambridge University Press, 1990.

[MRO 67] MROZ Z., "On the description of anisotropic workhardening", *J. Mech. Phys. Solids*, 15, p. 163, 1967.

[MUR 78] MURAKAMI S. and OHNO N., "A constitutive equation of creep damage in polycristalline metals", *I.U.T.A.M. Colloquium Euromech* 111, Marienbad, 1978.

[NEW 59] NEWMARK N.M., "A method of computation for structural dynamics", *A.S.C.E. Journal of Engineering Mechanics Division.*, Vol. 85, p. 67-94, 1959.

[ORT 86] ORTIZ M. and SIMO J.C., "An analysis of a new class of integration algorithms for elastoplastic constitutive relations", *Int. J. Numer. Meth., Eng.* Vol. 23, p. 353-366, 1986.

[QUE 98] QUEVAL J.C., COMBESCURE D., SOLLOGOUB P., COIN A. et MAZARS J., "CAMUS experimental program. In-plane tests of 1/3 scaled R/C bearing walls", *Proc. XIth ECEE-98*, CD-ROM eds Bisch P., Labbé P. et Pecker A., Paris/CNIT La defense, 1998.

[RAG 00] RAGUENEAU F., LA BORDERIE Ch. and MAZARS J., "Damage model for concrete like materials coupling cracking and friction, contribution towards structural damping: first uniaxial application", *Mechanics Cohesive Frictional Materials* (to appear), 2000.